DIFFERENTIAL SCANNING CALORIMETRIC STUDIES OF CO-PRECIPITATED MERCURY FERRITE

P D ZADE [a]* D.M. DHARMADHIKARI [b]
[a*]Dharampeth Education Society's Dharampeth Polytechnic, Ambazari, Nagpur
[b]CSIR-NEERI, Nehru Marg, Nagpur

A B S T R A C T

The differential scanning calorimetry (DSC) technique was used to analyse the thermal effects and the processes associated with the dehydration and properties of mercury ferrite powder co-precipitated from aqueous solution of salts obtained by simultaneous dissolution of mercuric chloride ($HgCl_2$) and ferrous sulphate ($FeSO_4.7H_2O$). Under optimum conditions of pH, temperature, Hg^{2+}/Fe^{2+} ratio and aeration rate, a mercury-bearing ferrite was obtained. An investigation into the crystalline structure of the ferrite by X-ray diffraction analysis (XRD) pointed to orthorhombic symmetry as the most probable structure similar to that of barium monoferrite. The electrical conductivity shows the semiconducting behaviour and suggests the use of synthesized material at high frequency on account of its high resistivity. Thermal measurement suggests the use at high temperatures, without any degradation.

Keywords: Oxide,Chemical Synthesis, Differential Scanning Calorimetry, X-ray Diffraction, Electrical Conductivity, Specific Heat

1. Introduction

The presence of water in co-precipitated mercury ferrite powders is a consequence of the precipitation mechanism and of the water chemisorption as a tendency of surface metal cations to complete the coordination with hydroxide ions.

The co-precipitation occurs through the condensation of neutral complex species, $\{[M^{z+}(H_2O)_{z-x}(OH)_x]^0$ and $[M^{z+}(OH)_z]^0\}$, which exist in aqueous solution of salts at basic pH values (Jolivet, Henry and Livage, 1994). The transition from soluble polynuclear species (precursors) to solid particles (homogeneous nucleation) occurs through formation of M–OH–M bridges (olation) and M–O–M bridges (oxolation), being accompanied by water loss (Musat Bujoreanu and Segal, 2001).

Depending on temperature of solution, the co-precipitated mercury ferrite powder contain variable amounts of water molecules and OH groups under various forms such as coordinated water (aqua- and hydroxo-complexes), constitutional water (hydroxides and oxyhydroxides) and lattice water, absorbed water into the pores and physically or chemisorbed water on the particle surface (Musat Bujoreanu and Segal, 2001, Lee, Newnhan, and Tye, 1973). These suggest the hygroscopic nature of the mercury ferrite formed.

Thus, the present work is based on the differential scanning calorimetric (DSC) study on dehydration of co-precipitated mercury ferrite (ferruginous mass) in relation to thermoanalytical measurements (TG-DTA), X-ray diffraction (XRD) and dc resistivity measurements is discussed.

The literature survey reveals that the mercury is a hazardous environmental contaminant. In Japan, 2252 people have been affected and 1043 have died due to minamata disease for the past three and half decades, caused by elevated mercury pollution from a chemical plant (Kudo and Miyahara, 1991).

It has been estimated that mercury emissions globally exceed 3000 tons annually (Schroeder and Munthe, 1998). The element can be found in air, sediments, soils, seawater, and freshwaters. Effects of the high levels of mercury in blood and hair can be correlated with sensory disturbances (paresthesia,

hypaesthesia), constriction of the visual field, hearing impairment, neurological disturbances (Sittig, 1995).

One of the main and more dangerous polluting sources for toxic elements is mercury containing wastewater, since it can be readily transported and spread into the environment. Hence, to keep the levels of mercury in the environment low, it is crucial to develop efficient procedures for wastewater decontamination, making sure that the residue generated as by-product is stable, resistant to further redissolution and can be used as a value added product.

The literature survey reveals that some of researchers (Wingenfelder, Hansen, Furrer, and Schulin, 2005, Anoop Krishnan, Anirudhan, 2002) have attempted the removal of mercury from water/wastewater and a few were successful. However, the disposal of sludge containing such toxic waste was a threat to the ecosystem. To overcome this problem, Zade et al (Zade and Dharmadhikari, 2006) have attempted to retrieve the mercury in the form of mercury ferrite as a value added product which could be used as a semiconductor owing to its activation energy resembles to the other semiconducting compounds in use. The mercury ferrite may also be used at high frequency because of its high resistivity. Thermal analysis of the synthesized compound shows that the compound is thermally stable.

The present study shows that the transition temperature observed in DSC is similar to that of electrical conductivity measurements.

Generally, ferrites have low Curie temperature (Tc) and their magnetization may fluctuate upon temperature variation in ultra high frequency range. Also due to their magneto-crystalline anisotropy, the frequency range of some ferrites is limited by the occurrence of ferromagnetic resonance (FMR), the so called Snoek's limitation (Chikazumi, 1997). Therefore, properties like thermal stability and electrical conductivity in terms of power dissipations need particular attention.

2. Experimental

The mercury ferrite powder was co-precipitated at 323 ± 1 K. The co-precipitation was achieved by giving the optimum dose of ferrous sulphate ($FeSO_4.7H_2O$) to the solution containing Hg^{2+} ions at an optimum pH = 10.0, value. The pH was maintained by the addition of 1N solution of sodium hydroxide (NaOH) and the solution is then aerated at the aeration rate of 100 ml/min which was adjusted with precalibrated gap kit meter into the solution until the black magnetic ferrite is formed. The mercury ions in filtrate and the sludge were determined by Cold Vapor Atomic Absorption Spectrophotometer (CVAAS) (Eaton, Clesceri, Rice. and Greenberg, 2005) and total iron in filtrate and the sludge were estimated by 1, 10 Phenanthroline spectrophotometric method (Eaton, Clesceri, Rice. and Greenberg, 2005) and atomic absorption spectrophotometer (AAS) (Make: GBC 904 AA, Australia) (Eaton, Clesceri, Rice. and Greenberg, 2005).

2.1. Characterization

Thermoanalytical measurements (TG-DTA) of mercury ferrite from room temperature to 1173 K have been performed by a Seiko thermogravimetric analyser at a heating rate of 10 K min^{-1}. The inert reference was α- Al_2O_3 (Model: TG/DTA-32).

DSC analyses were performed on mercury ferrite by a Mettler Toledo differential scanning calorimeter (Model: DSC821e) from room temperature to 673 K at a heating rate of 10 K min^{-1} in an air stream and a suitable amount of sample (~10 mg). The standard alumina crucibles were used for the analysis.

X- ray diffraction studies on mercury ferrite were carried out with a Philips Analytical Diffractometer (Make: Philips, X'Pert PRO) from 10 degree to 60 degree using $CuK\alpha_1$ radiation (λ=1.5404).

dc resistivity of mercury ferrite was measured from room temperature to 773 K using specially fabricated sample holder, which ensures smooth contact of electrodes with the surface of the pellets. The temperature was facilitated by the use of cromel/alumel thermocouple which was connected to sample holder appropriately. The two electrodes of sample holder were connected to million-mega ohm meter/LCR meter.

3. Results and discussion

Thermogravimetric analysis of the co-precipitated mercury ferrite (Zade and Dharmadhikari, 2006) has shown in figure 1, reveals considerable mass loss, depending on the temperature for the sample.

In the temperature range 303 – 673 K, about 11% of this mass loss occurs and as the temperature was increased to 1083.6 K, the mass loss has slightly increased to 14.2 %,

corresponds to the temperature of 1083.6 K. Thus, from the temperature range 673 K – 1083.6 K, only a mass loss of 3.4 % is detected by thermogravimetric curve (TG) and differential thermal analysis (DTA) curves, this overall process results indicate that there was no other volatile component; the mass loss is to be assigned exclusively to the water loss.

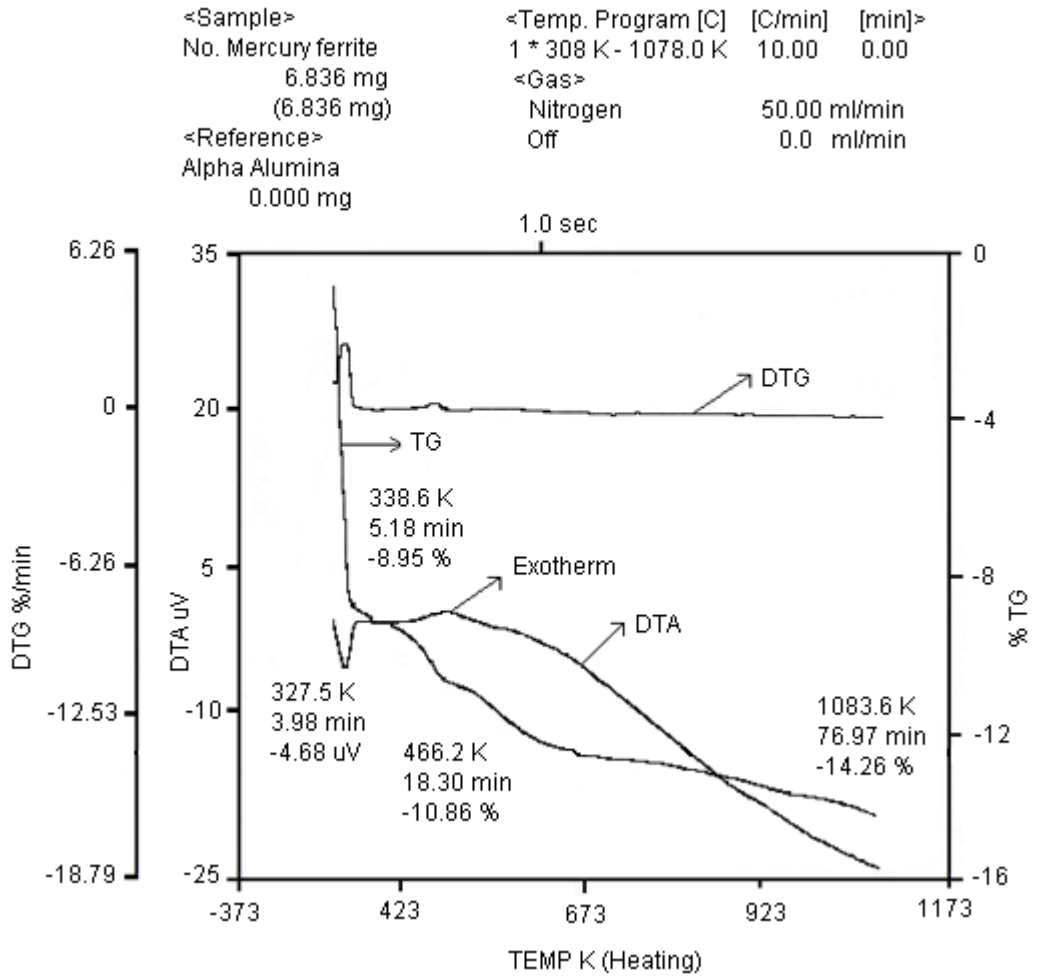

Figure-1. Thermo gravimetric (TG) and differential thermal analysis (DTA) pattern of mercury ferrite

Figure 2 shows the differential scanning calorimetric (DSC) curve of the mercury ferrite which demonstrates two broad endothermic peaks, one at 388 K and the other at 552.24 K in the temperature ranges of 313 K – 393 K and 393 – 573 K respectively. It seems evident to consider these peaks at 388 K and 552.24 K corresponds to the elimination of the physically adsorbed water molecules with various degrees of structuration via hydrogen bonds.

The first endothermic peak at 327.5 K in thermogravimetric and differential thermal analysis curve of mercury ferrite (figure 1) is shifted to lower temperature as compared to the endothermic peak at 329.4 K of magnetite (figure 3). In differential scanning calorimetric (DSC) curve (figure 2), the first endothermic peak at 383 K corresponds to the exclusion of the moisture content, this shift of first endothermic peak to higher temperature could be explained as lower the temperature of co-precipitation is, the higher the temperature is, at which the first peak is shifted. The second exothermic peak relates to the removal of the lattice water and the water from the pores. In the case of the third exothermic peak, the superposition of some slight exothermic processes in the range 613 K – 635 K can be observed if the temperature increases (Musat Bujoreanu, Segal, 2002).

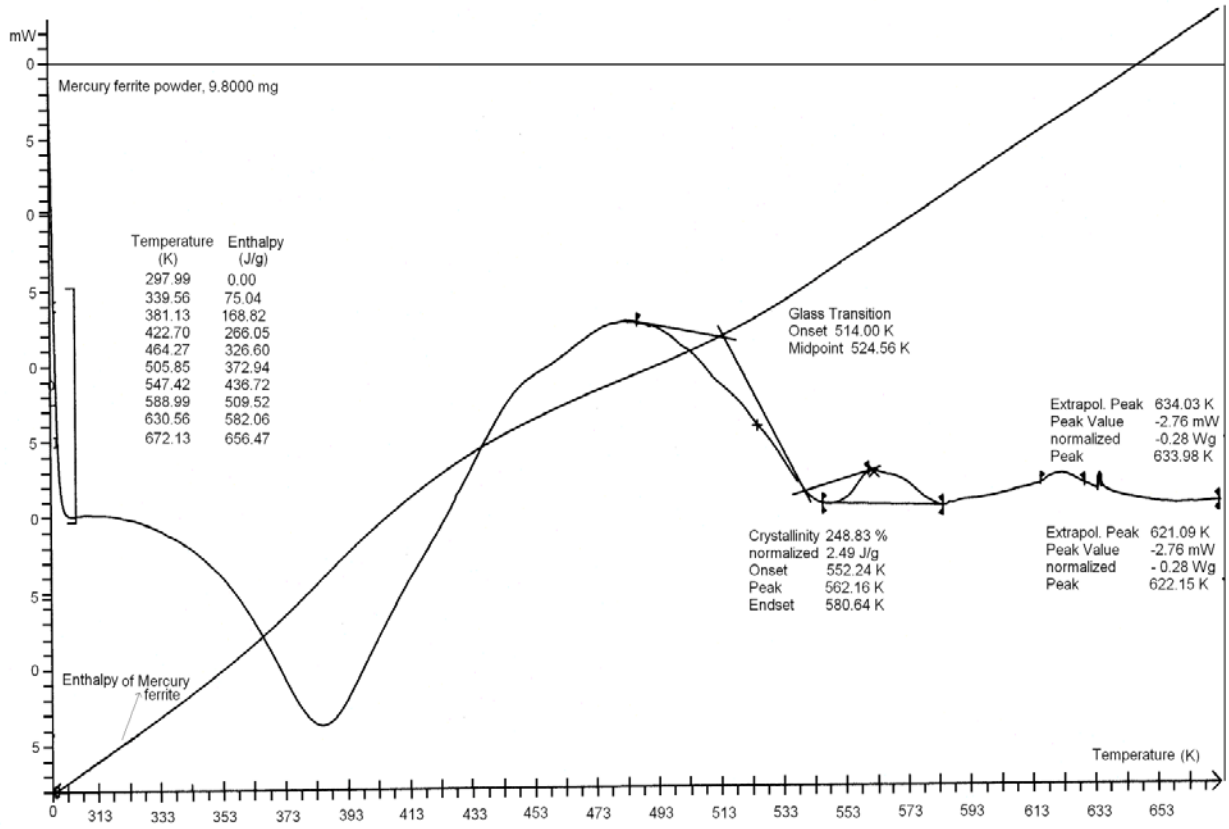

Figure-2 Differential scanning calorimetric studies (DSC) pattern of mercury ferrite

The exothermic peak at 524.56 K on the DSC curves shows the glass transition temperature of mercury ferrite which suggests the subtle phase change and is associated with a slight mass loss and weak exothermic peaks on the TG and DTA curves as reported by Musat Bujoreanu for manganese ferrite (Musat Bujoreanu, Segal, 2001). This exothermic peak corresponds to the microstructure changes associated with the elimination of water from the micropores. The removal of water is accompanied by a decrease of the number of point defects, by the formation of (111) and (422/620) planes, these planes are observed in the X-ray diffraction pattern of mercury ferrite (figure 4) and the sharp peak in X-ray diffraction pattern indicates that the larger crystallite size as reported by Musat Bujoreanu for manganese ferrite (Musat Bujoreanu, Segal, 2001). The increase of crystallite size could also be explained on the basis of M-O-M bridges which forms the framework of spinel lattice of magnetite and are responsible for the elimination of pores which leads to the increase of crystallite size and healing of the point defects as a results of incorporation of Hg^{2+} ions, the peak at 562.16 K in DSC curve further confirms this.

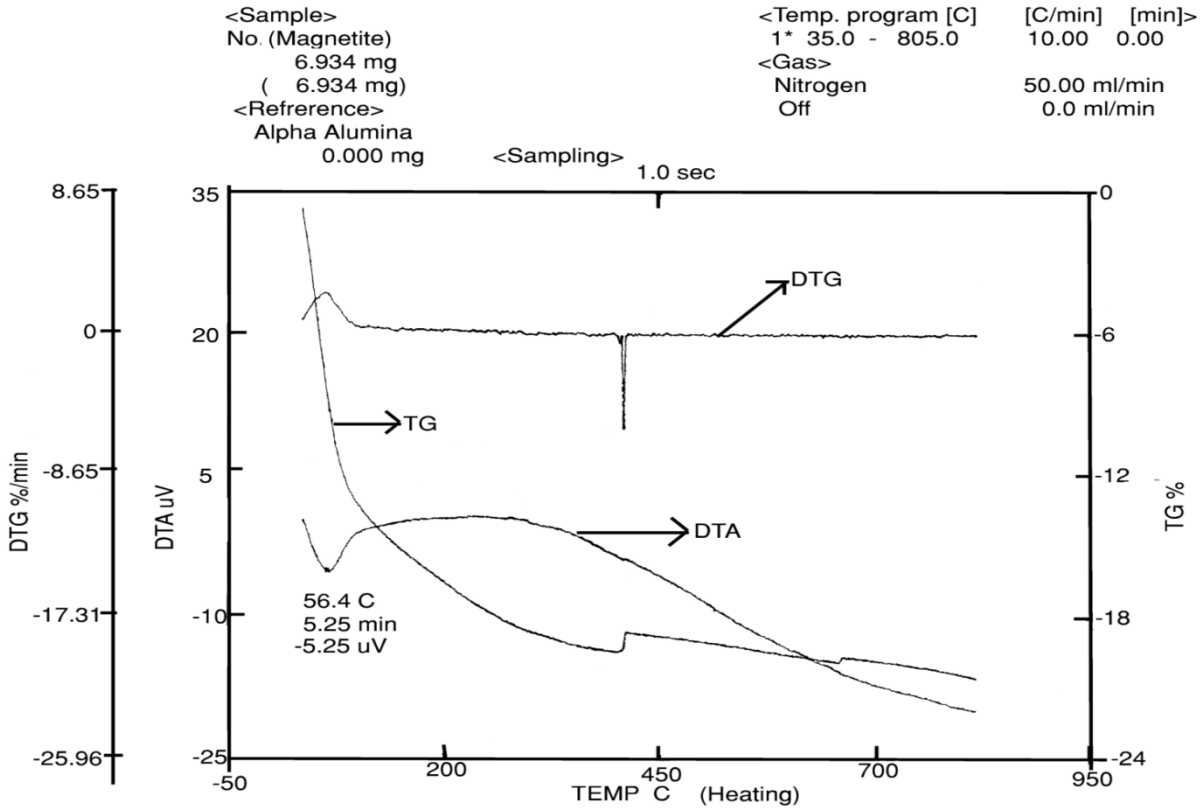

Figure-3 Thermogravimetric (TG) and differential thermal analysis pattern of magnetite (Fe_3O_4)

Figure 2 clearly show that if until ~ 423 K an endothermic effect is recorded, at higher temperatures this is partly compensated by exothermic ones. The DTA curve in figure 1 in these temperature ranges further supports this. The lower the water amount from powder is, the more extended the exothermic effect corresponding to the structuration of the lattice is.

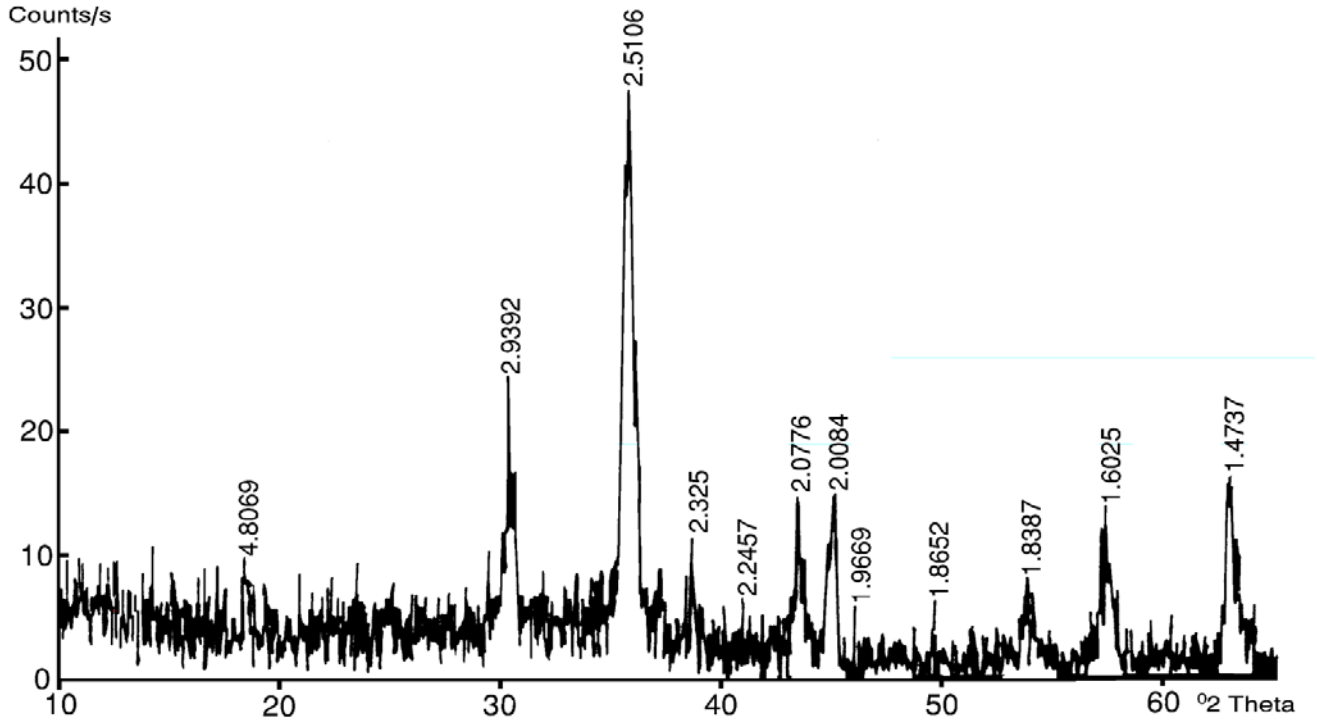

Figure-4 X-ray diffraction pattern of mercury ferrite

The other broad exothermic effects at temperature 562.16 K and 634.03 K, these bands may be assigned to the transition from mixed metal hydroxide to the well crystallized orthorhombic symmetry as revealed by XRD and as reported by Lo´pez-Delgado Aurora for nickel – chromium – zinc ferrite (Lo´pez-Delgado, Lo´peza Felix, Vidales Jose'L and Vila Eladio, 1999). The room temperature X-ray diffraction pattern shows close resemblance to barium monoferrite structure with unit cell parameter as a = 19.10 Å b = 6.019 Å, c = 8.164 Å. No peaks attributable to other phases/ parent compounds were observed in the diffractograms. The transition phenomenon of spinel to orthorhombic could be assigned to the breaking of M-OH-M bond and reforming of M-O-M bonds corresponding to the release of the water. This theory is supported and confirmed during the calcination in air at temperatures higher than 473 K in DSC curve, the removal of water is accompanied by a slight reorganization and relaxation of spinel lattice of magnetite. The observation agrees with the X-ray diffraction pattern in figure 4 which shows the compound crystallizing in orthorhombic symmetry and sharp peak, suggesting the characteristics of crystalline material.

Another broad exothermic peak at 622.15 K is the phase transition temperature, which is observed in the electrical conductivity measurement as presented in figure 5 as the Curie temperature ($Tc_{elect.}$ = 615.23 ± 10 K) and can be attributed responsible for the transition of ferrimagnetic state to paramagnetic state (Sattar, El-Sayed, El-Shokrofy and El-Tabey, 2007) and the change in the conduction mechanism (Murthy and Sobhandri, 1976). Figure 5 shows the variation of resistivity with increase in temperature, initially resistivity decreases upto 615 K and thereafter the resistivity increases further with increase in temperature; the increase in resistivity, the value of activation energy (2.46 eV) also increased because it can also been seen that samples having high resistivity have high activation energy as reported by other researchers (Islam, Ahmed, Abbas and Choudhary, 1999, Islam, Ashraf, Abbas, Umar, 1997, El-Shabasy, 1997).

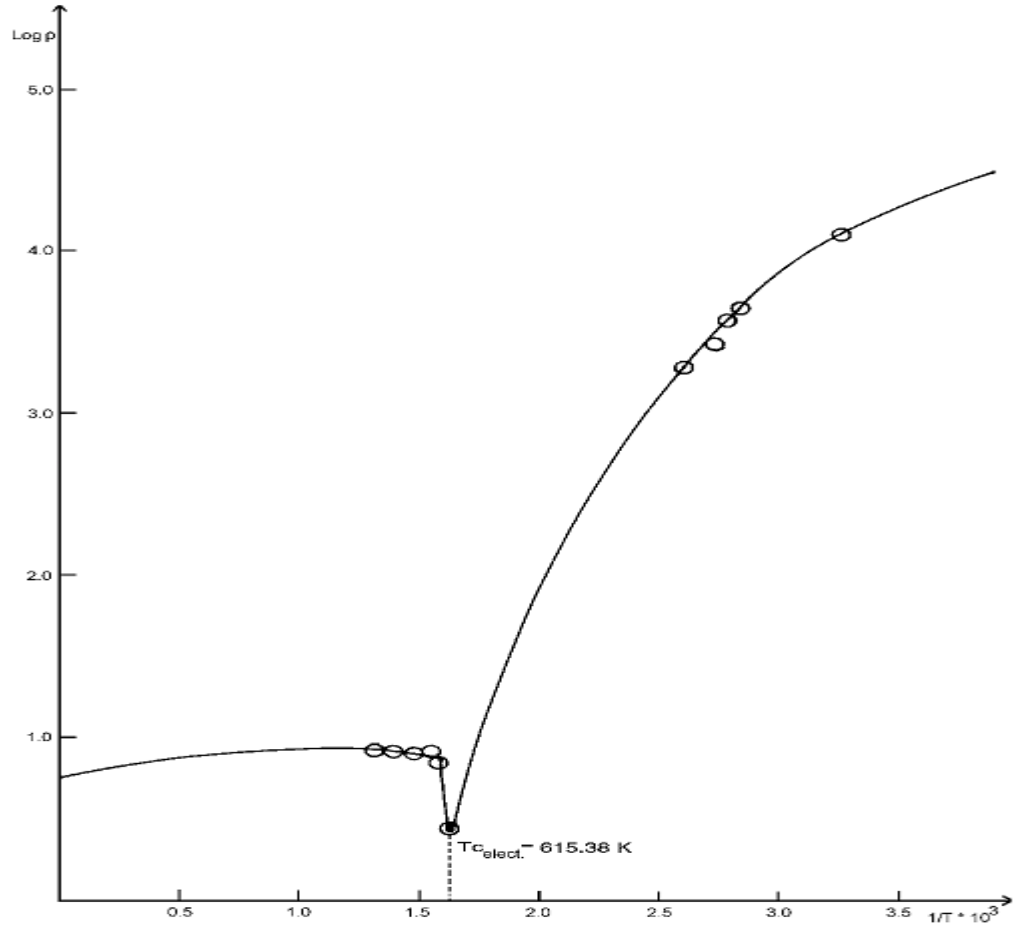

Figure-5 dc resistivity of mercury ferrite

Drift mobility of the synthesized compound has been calculated using the equation (1) (Islam, Ahmed, Abbas and Choudhary, 1999):

$$\mu = 1/ ne\rho \quad (1)$$

Where 'e' is the charge on electron, 'ρ' is the resistivity and 'n' is the concentration of charge carriers, which can be calculated from the following equation (2) (Islam, Ahmed, Abbas and Choudhary, 1999):

$$n = N_a \rho_a P/ M \quad (2)$$

Where 'M' is the molecular weight, 'N_a' the Avogadro's number, 'ρ_a' the density of Sample (5.65 ± 0.025 gm/cm^3) and 'P' = 2 is the number of iron atoms in the chemical formula of the oxide.

The value of drift mobility ($9.03 * 10^{-11}$ m^2/V-s) calculated from the equation 1 and 2 (Islam, Ahmed, Abbas and Choudhary, 1999, Islam, Ashraf, Abbas and Umar, 1997) shows that the compound having high resistivity have low mobility.

It is observed that by increasing temperature mobility also increases. It may be due to the fact that the charge carriers start hopping from one site to another as temperature increases, as reported by other researchers (Islam, Ahmed, Abbas and Choudhary, 1999, Islam, Ashraf, Abbas, Umar, 1997).

The specific heat was calculated using the formula (3):

$$q = (\text{mass})\ (\delta t)\ (C_p) \quad (3)$$

where, 'δt' is the change in temperature from start to finish in degrees Kelvin, 'm' is the mass of substance in grams, 'C_p' is the specific heat. Its unit is Joules per gram-degree Kelvin (J / g K is one way to write the unit; J g^{-1} K^{-1} is another), 'q' is the amount of heat involved, measured in Joules or kilojoules (symbols = J and kJ).The numerical calculations of specific heat from the equation 3 and the enthalpy are indicated in Table 1. From Table 1, it is clear that the difference of specific heat (ΔCp) decreases before glass transition temperature (Tg) with increase in temperature and subsequently an increase in difference of specific heat (ΔCp) is observed, which specify that the ΔCp should decrease monotonically as nonmagnetic atoms are substituted for magnetic atoms on the A sites. On the other hand, if the nonmagnetic atoms go on the B sites, ΔCp should pass through a maximum (Howard and Samual smart, 1953). Thus, result suggests the preference of Hg^{2+} ions on the B sites.

Table 1 - Specific heat of mercury ferrite obtained from the enthalpy data in DSC

Sr. No.	Temperature (K)	Enthalpy (H) J g^{-1}	Specific heat (Cp) J/g K
1.	297.99	0.00	[a]
2.	339.56	75.04	184.37
3.	381.13	168.82	414.79
4.	422.70	266.05	653.68
5.	464.27	326.60	802.45
6.	505.85	372.94	916.31
7.	547.42	436.72	1073.02
8.	588.99	509.52	1251.89
9.	630.56	582.06	1430.12
10.	672.13	656.47	1612.94

[a]Value not obtained

4. Conclusions

The mercury ferrite may be used at high temperature applications because of its thermal stability. The high resistivity of our synthesized mercury ferrite is useful for the minimization of eddy current losses (Verma, Goel, Mendiratta and Gupta, 1999). The temperature dependent mobility increases with the increase of temperature whereas resistivity decreases; this may be attributed to the semi conducting behavior of the mercury ferrite.

The enthalpy/ heat content and specific heat of mercury ferrite formation starting from the constituent oxides have been estimated. It is observed to be increasing. The synthesis process developed for the preparation of

mercury ferrite is a low cost and eco-friendly technology that allows total recovery of mercury in the form of ferruginous material, a value added product as mercury ferrite.

Acknowledgement

The authors are thankful to Shri Shreedhar Gadge, Vishweshwarya National Institute of Technology, Nagpur India, for providing facilities to carry out differential scanning calorimetric studies. The authors also wish to thank Dr. Shirish Pradhan, National Chemical Laboratory, Pune, India and Dr. Anand Aswar, Amravati University, Amravati, India for providing the facilities for X-ray diffraction, thermal analysis and dc Resistivity measurements.

References

1. Jolivet J.P., Henry M, Livage J. (1994) *Condensation of Cations in Aqueous Solution, Oxide Surface Chemistry*, Savoirs Actuels, Inter Editions et CNRS Ed., Paris.

2. Musat Bujoreanu V., Segal E., (2001), On the dehydration of mixed oxides powders co-precipitated from aqueous solutions, *Solid State Sci.* 3, 407– 415.

3. Lee J.A., Newnhan C.E., and Tye F.L., (1973), Energetics of water desorption from a γ-manganese dioxide, *J. Colloid Interface Sci*. 42(2), 372–380.

4. Kudo A., Miyahara S., (1991), A case history; Minamata mercury pollution in Japan-from loss of human lives to decontamination, *Water Sci. Technol*. 23, 283–290.

5. Schroeder W.H., Munthe J., (1998), Atmospheric mercury - an overview, *Atmos. Environ*. 32 (5), 809–822.

6. Sittig M., (1995), *Handbook of Toxic and Hazardous Chemicals and Carcinogens*, II nd ed., Noyes Publications, New York, pp. 569–572.

7. Wingenfelder U., Hansen C., Furrer G., and Schulin R., (2005), Removal of heavy metals from mine waters by natural zeolites, *Environ. Sci. Technol.* 39(12), 4606–4613.

8. Anoop Krishnan K., Anirudhan T.S., (2002), Removal of mercury (II) from aqueous solutions and chlor-alkali industry effluent by steam activated and sulphurised activated carbons prepared from bagasse pith: kinetics and equilibrium studies, *J. Hazard. Mater*. 92(2), 161–183.

9. Zade P.D., Dharmadhikari D.M., and Kulkarni D.K., (2006), Crystal structure of $HgFe_2O_4$, *Current Sci*. 91(2), 157.

10. Chikazumi S. (Eds.), (1997), *Physics of Ferromagnetism*, II nd ed., Oxford University Press, New York.

11. Eaton A.D., Clesceri L.S., Rice E.W., and Greenberg A.E., (2005), *Standard Methods for the Examination of Water and Wastewater*, American Public Health Association (APHA), New York, 21 st Edition.

12. Musat Bujoreanu V., Segal E., (2002), DSC study of water elimination from the co-precipitated ferrite powders, *J. Therm. Anal. Calorim*. 68(1), 191–197.

13. Lo´pez-Delgado Aurora, Lo´peza Felix A., Vidales Jose´ L Martı´n de., and Vila Eladio, (1999), Synthesis of nickel–chromium–zinc ferrite powders from stainless steel pickling liquors, *J. Mater.Res.* 14(8),3427–3432.

14. Sattar A.A., El-Sayed H.M., and El-Shokrofy K.M., and El-Tabey M.M., (2007), Study of the dc resistivity and thermoelectric power in Mn-substituted Ni–Zn ferrites, *J. Mater. Sci*. 42, 149–155.

15. Murthy V.R.K, Sobhanadri J., (1976), Electrical conductivity of some nickel-zinc ferrites**,** *Phys. Stat. Sol.* (a). 38(2), pp. 647 – 651.

16. Islam M.U., Ahmad I., Abbas T., and Chaudhry M.A., (1999), Proceedings of the Sixth International Symposium on Advanced Materials, Islamabad, Pakistan, 155– 158.

17. Islam M.U., Ashraf Chaudhry M., Abbas T., and Umar M., (1997) Temperature dependent electrical resistivity of Co–Zn–Fe–O system, *Mater. Chem. Phys*. 48 227–229.

18. El-Shabasy M., (1997), DC electrical properties of Ni-Zn ferrites, *J. Magn. Magn. Mater*. 172, 188–192.

19. Howard L.N., Samuel Smart J., (1953), The specific heat discontinuity in antiferromagnets and ferrites, *Phys. Rev*. 91, 17–19.

20. Verma A., Goel T.C., Mendiratta R.G., and Gupta R.G., (1999), High-resistivity nickel–zinc ferrites by the citrate precursor method, *J. Magn. Magn. Mater*. 192(2), 271–276.